Research Article

Electrophoresis of a Sphere along the Axis of a Cylindrical Pore: Effects of Double-Layer Polarization and Electroosmotic Flow

Jyh-Ping Hsu, and Zheng-Syun Chen

Langmuir, **2007**, 23 (11), 6198-6204 • DOI: 10.1021/la070079m

Langmuir

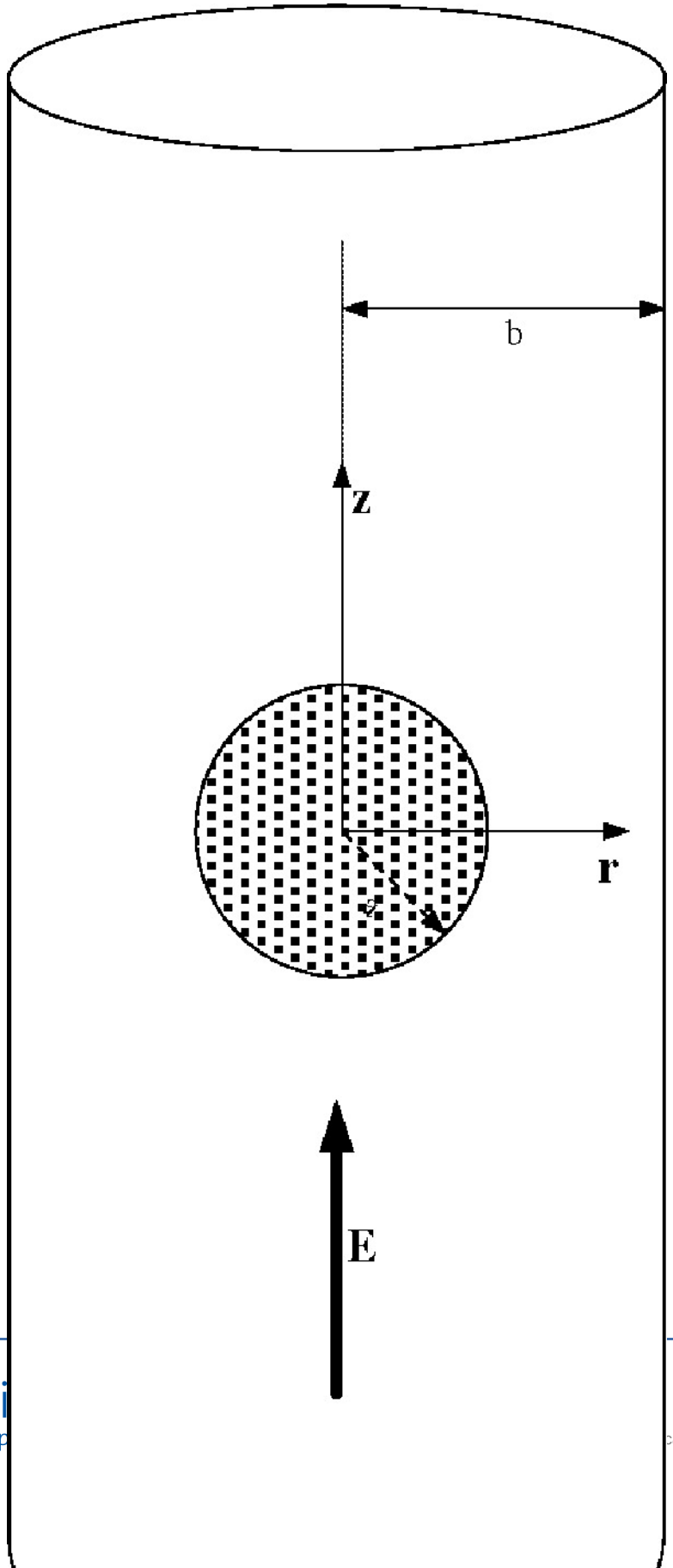

Electrophoresis of a Sphere along the Axis of a Cylindrical Pore: Effects of Double-Layer Polarization and Electroosmotic Flow

Jyh-Ping Hsu* and Zheng-Syun Chen

Department of Chemical Engineering, National Taiwan University, Taipei, Taiwan 10617

Received January 11, 2007. In Final Form: March 9, 2007

The electrophoresis of a rigid sphere along the axis of a cylindrical pore is investigated theoretically. Previous analysis is extended to the case where the effects of double-layer polarization and electroosmotic flow can be significant. The influences of the surface potential, the thickness of the double layer, and the relative size of a pore on the electrophoretic behavior of a sphere are discussed. Some interesting results are observed. For example, if both a sphere and a pore are positively charged, then the mobility of the sphere has a local minimum as the thickness of its double layer varies. Depending upon the level of the surface potential of a sphere and the degree of significance of the boundary effect, the mobility of the sphere may change its sign twice as the thickness of its double layer varies. This result can play a significant role in electrophoresis measurements.

1. Introduction

Electrophoresis has many applications in various fields. It is not only adopted often to characterize the charged conditions of entities of colloidal size but also used widely in both conventional and modern operations. One of the key effects in conducting electrophoresis and electrophoresis-related operations is the presence of a boundary. Electrophoresis conducted in a narrow space such as capillary electrophoresis is a typical example of the former, and electrodeposition where charged particles are driven by an applied electric field toward electrodes is an example of the latter. The charged conditions on a boundary can make things even more complicated because the associated electroosmotic flow will influence not only the magnitude of the electrophoretic velocity of a particle but also its direction.

The boundary effect on electrophoresis has been studied extensively in the last few decades, and various types of problems have been investigated. These include the electrophoresis of a sphere parallel to a plate,[1−4] along the axis of a cylindrical pore,[2−6] positioned eccentrically in a cylindrical pore,[7−9] through a converging-diverging pore,[10] along the center line between two parallel plates,[2,4] and in a spherical cavity.[11−14] Although the presence of a boundary simply yields an extra viscous force on a particle arising from the nonslip condition on the boundary, the influences of other effects such as the level of surface potential, the thickness of the electrical double layer, and the charged conditions on the boundary surface can be profound. For instance, if a boundary is charged, an electroosmotic flow is generated that will influence both qualitatively and quantitatively the electrophoretic behavior of a particle.[2] The interaction between the double layer of a particle with a boundary can also lead to complicated results.[6]

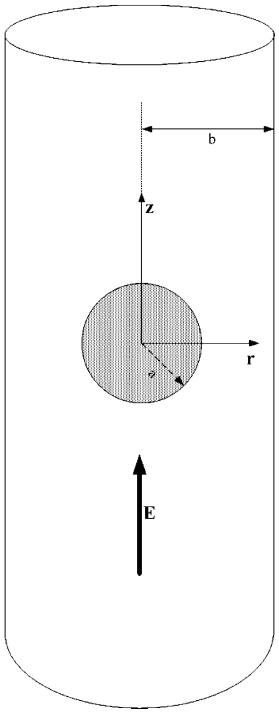

Figure 1. Schematic representation of the problem considered where a sphere of radius *a* is placed on the axis of a long cylindrical pore of radius *b*. A uniform electric field **E** parallel to the axis of the pore is applied. The cylindrical coordinates (r, θ, z) with the origin located at the center of the sphere are adopted.

In this study, previous analysis of the electrophoresis of a sphere along the axis of a cylindrical pore under the conditions of low surface potential and weak applied electric field[6] is extended to the case of arbitrary surface potential and double-layer thickness. Also, the surface of a sphere and that of a pore can be charged. This implies that the effects of double-layer polarization and electroosmostic flow, both of practical significance,[15−16] can be important and should be taken into account.

* To whom correspondence should be addressed. E-mail: jphsu@ntu.edu.tw. Fax: 886-2-23623040.

(1) Keh, H. J.; Chen, S. B. *J. Fluid Mech.* **1988**, *194*, 377.
(2) Keh, H. J.; Anderson, J. L. *J. Fluid Mech.* **1985**, *153*, 417.
(3) Shugai, A. A.; Carnie, S. L. *J. Colloid Interface Sci.* **1999**, *213*, 298.
(4) Ennis, J.; Anderson, J. L. *J. Colloid Interface Sci.* **1997**, *185*, 497.
(5) Keh, H. J.; Chiou, L. C. *Am. Inst. Chem. Eng. J.* **1996**, *42*, 1397.
(6) Hsu, J. P.; Ku, M. H. *J. Colloid Interface Sci.* **2005**, *283*, 592.
(7) Yariv, E.; Brenner, H. *Phys. Fluids* **2002**, *14*, 3354.
(8) Ye, C.; Xuan, X.; Li, D. *Microfluid Nanofluid* **2005**, *1*, 234.
(9) Hsu, J. P.; Kuo, C. C. *J. Phys. Chem. B* **2006**, *110*, 17607.
(10) Davison, S. M.; Sharp, K. V. *J. Colloid Interface Sci.* **2006**, *303*, 288.
(11) Zydney, A. L. *J. Colloid Interface Sci.* **1995**, *169*, 476.
(12) Lee, E.; Chu, J. W.; Hsu, J. P. *J. Colloid Interface Sci.* **1997**, *196*, 316.
(13) Lee, E.; Chu, J. W.; Hsu, J. P. *J. Colloid Interface Sci.* **1998**, *205*, 65.
(14) Hsu, J. P.; Hung, S. H.; Kao, C. Y. *Langmuir* **2002**, *18*, 8897.

10.1021/la070079m CCC: $37.00
Published on Web 05/01/2007

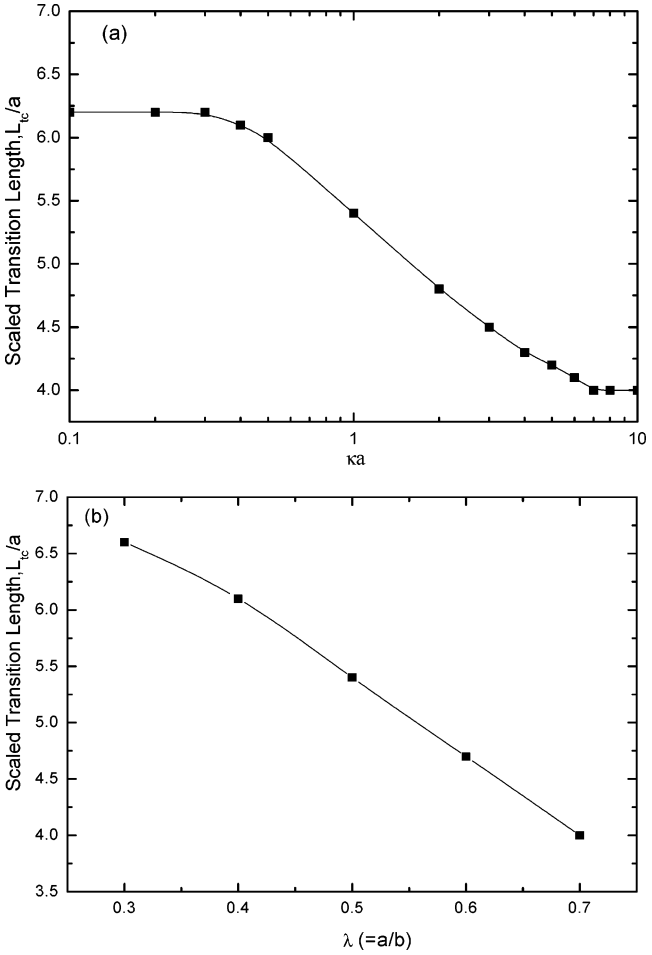

Figure 2. Variation of the scaled transition length (L_{tc}/a) (a) as a function of κa at $\phi_r = \zeta_a z_1 e/k_B T = 1$, $\zeta^*_b = 0.2\zeta^*_a$, and $\lambda = 0.5$ and (b) as a function of λ ($= a/b$) at $\phi_r = 1$, $\zeta^*_b = 0.2\zeta^*_a$, and $\kappa a = 1$.

2. Theory

Let us consider the electrophoresis of a rigid sphere of radius a along the axis of a long cylindrical pore of radius b shown in Figure 1. The liquid phase is an incompressible Newtonian fluid with constant physical properties. The cylindrical coordinates (r, θ, z) are chosen with the origin located at the center of the sphere. A uniform electric field **E** is applied in the z direction, and **U** is the corresponding electrophoretic velocity of the sphere. The symmetric nature of the system under consideration suggests that only the (r, z) domain has to be considered. For the present case, the electrical potential ϕ can be described by the Poisson equation

$$\nabla^2\phi = -\frac{\rho}{\epsilon} = -\sum_j^2 \frac{z_j e n_j}{\epsilon} \qquad (1)$$

Here, ∇^2 is the Laplace operator, ϵ is the permittivity of the liquid phase, ρ is the space charge density, e is the elementary charge, and n_j and z_j are the number concentration and the valence of ionic species j, respectively. If we let D_j, k_B, T, and **v** be the diffusivity of ionic species j, the Boltzmann constant, the absolute temperature, and the liquid velocity, respectively, then the conservation of ionic species at steady state leads to

$$\nabla\cdot\left[-D_j\left(\nabla n_j + \frac{z_j e}{k_B T} n_j \nabla\phi\right) + n_j \mathbf{v}\right] = 0 \qquad (2)$$

For convenience, ϕ is decomposed into an equilibrium potential or the potential in the absence of **E**, ϕ_1, and a perturbed potential

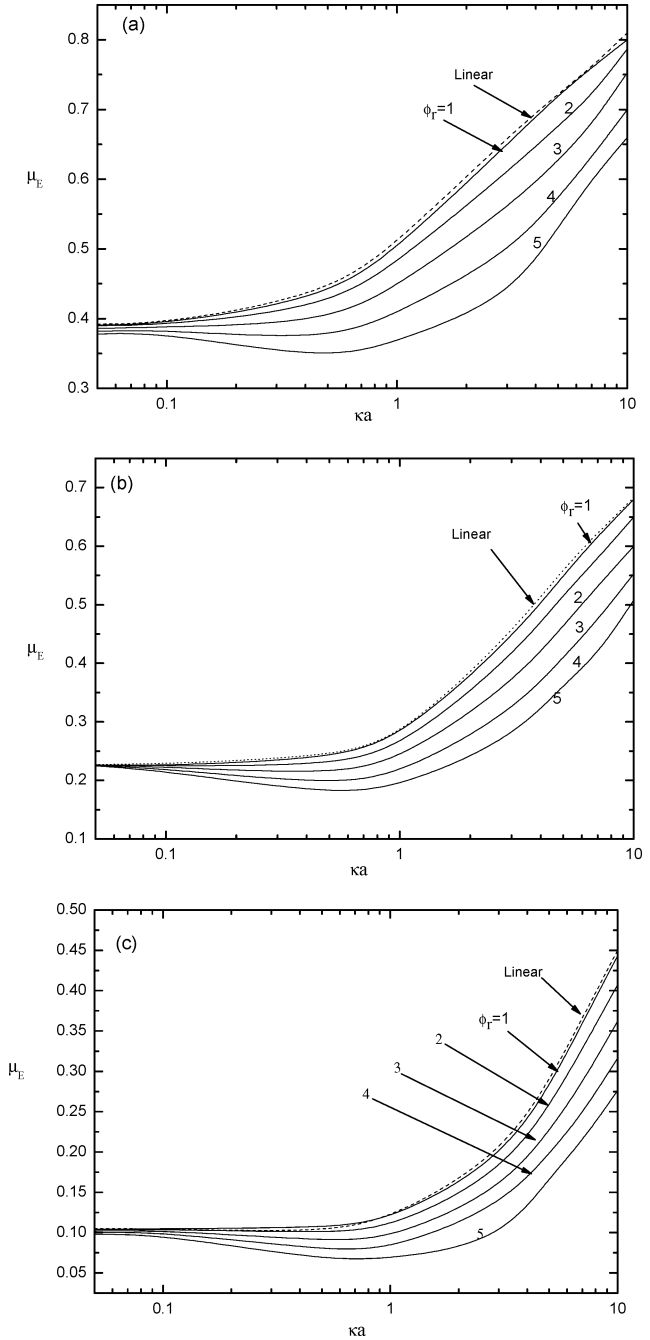

Figure 3. Variation of the scaled electrophoretic mobility μ_E (defined in eq 28) as a function of κa at various levels of ϕ_r ($= \zeta_a z_1 e/k_B T$) for the case of $\zeta^*_b = 0$. (a) $\lambda = 0.3$, (b) $\lambda = 0.5$, and (c) $\lambda = 0.7$.

(15) Wong, P. K.; Wang, T. H.; Deval, J. H.; Ho, C. M. *IEEE-ASME Trans. Mech.* **2004**, *9*, 366.
(16) Stone, H. A.; Stroock, A. D.; Ajdari, A. *Annu. Rev. Fluid Mech.* **2004**, *36*, 381.
(17) Wiersema, P. H.; Loeb, A. L.; Overbeek, J. Th. G. *J. Colloid Interface Sci.* **1966**, *22*, 78.

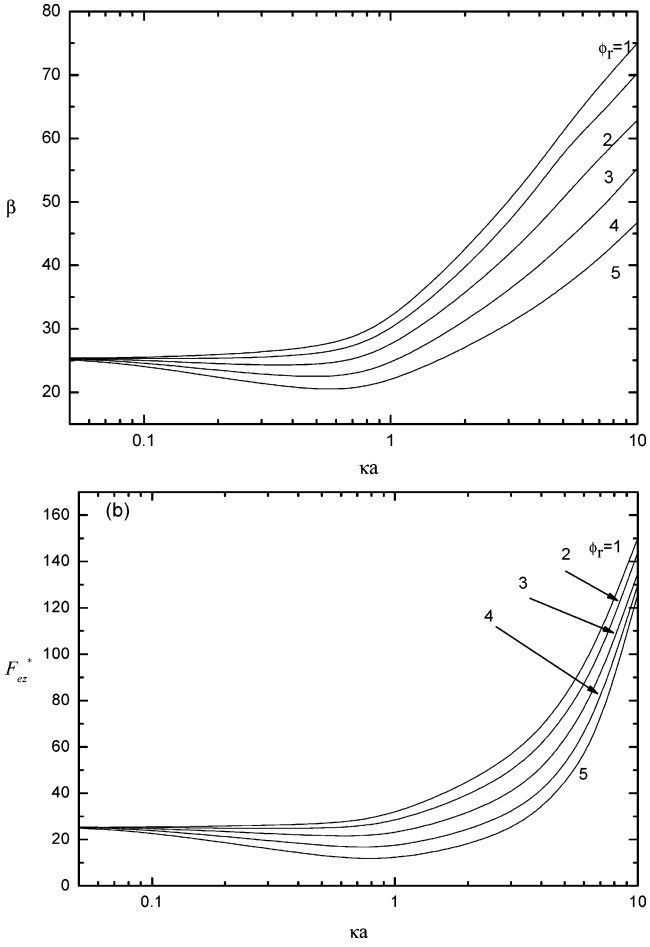

Figure 4. (a) Variation of β (defined in eq 27) as a function of κa at various levels of ϕ_r ($= \zeta_a z_1 e/k_B T$) and (b) that of F^*_{ez} (defined in eq 31) as a function of κa for the case when $\zeta^*_b = 0$ and $\lambda = 0.5$.

arising from **E**, ϕ_2, that is, $\phi = \phi_1 + \phi_2$.[18] Also, n_j is expressed as[18]

$$n_j = n_{j0} \exp\left(-\frac{z_j e(\phi_1 + \phi_2 + g_j)}{k_B T}\right) \tag{3}$$

where g_j is a perturbed potential that takes account of the deformation of the double layer surrounding a particle as it moves. Note that the form of eq 3 is assumed for convenience. Until now, g_j has been considered to be an arbitrary function. Under conditions of practical significance, the applied electric field is weak compared with that established by the sphere and/or by the cavity so that the expressions for the distortion of the double layer, the electric potential, and the flow field near the sphere can be linearized. For example, the scaled number concentrations of ions, n^*_1 and n^*_2, can be approximated respectively by

$$n^*_1 = \exp(\phi_r \phi^*_1)[1 - \phi_r(\phi^*_2 + g^*_1)] \tag{4}$$

$$n^*_2 = \exp(\alpha\phi_r \phi^*_1)[1 + \alpha\phi_r(\phi^*_2 + g^*_2)] \tag{5}$$

where $n^*_j = n_j/n_{10}$, $\phi^*_j = \phi_j/\zeta_a$, $g^*_j = g_j/\zeta_a$, $j = 1, 2$, $\alpha = -z_2/z_1$, $\phi_r = \zeta_a z_1 e/k_B T$, and ζ_a is the surface potential of the sphere. In scaled quantities, the equilibrium electrical potential can be described by

$$\nabla^{*2}\phi^*_1 = -\frac{1}{(1+\alpha)}\frac{(\kappa a)^2}{\phi_r}[\exp(-\phi_r\phi^*_1) - \exp(\alpha\phi_r\phi^*_1)] \tag{6}$$

where $\nabla^{*2} = \nabla^2/a^2$ is the scaled Laplace operator and $\kappa = [\sum_{j=1}^{2} n_{j0}(ez_j)^2/\epsilon k_B T]^{1/2}$ is the reciprocal Debye length. It can be shown that eqs 1, 3, 4, 5, and 6 lead to

$$\nabla^{*2}\phi^*_2 - \frac{(\kappa a)^2}{(1+\alpha)}[\exp(-\phi_r\phi^*_1) + \alpha\exp(\alpha\phi_r\phi^*_1)]\phi^*_2 = \frac{(\kappa a)^2}{(1+\alpha)}[\exp(-\phi_r\phi^*_1)g^*_1 + \exp(\alpha\phi_r\phi^*_1)\alpha g^*_2] \tag{7}$$

after neglecting terms involving products of small quantities such as g^*_1, g^*_2, and ϕ^*_2. Similarly, the variation of g^*_j can be approximated by employing eqs 3−5 to obtain

$$\nabla^{*2}g^*_1 - \phi_r\nabla^*\phi^*_1\cdot\nabla^* g^*_1 = \phi_r{}^2 Pe_1 \mathbf{v}^*\cdot\nabla^*\phi^*_1 \tag{8}$$

$$\nabla^{*2}g^*_2 - \alpha\phi_r\nabla^*\phi^*_1\cdot\nabla^* g^*_2 = \phi_r{}^2 Pe_2 \mathbf{v}^*\cdot\nabla^*\phi^*_1 \tag{9}$$

Here, $\nabla^* = \nabla/a$ is the scaled gradient operator, $\mathbf{v}^* = \mathbf{v}/U_E$, $U_E = \epsilon\zeta_a{}^2/\eta a$ is the magnitude of the velocity based on Smoluchowski's theory when an electric field of strength ζ_a/a is applied, η is the viscosity of the liquid phase, and $Pe_j = \epsilon(z_j e/k_B T)^2/\eta D_j$ for $j = 1, 2$ is the electric Peclet number of ionic species j.

We assume that both the sphere and the pore are nonconductive, impermeable to ionic species, and remain at constant surface potential. Also, the concentrations of ionic species reach the bulk values at both the inlet and the outlet of a pore. These lead to the following boundary conditions:

$$\phi^*_1 = \frac{\zeta_a}{\zeta_a} \text{ on the sphere surface} \tag{10}$$

$$\phi^*_1 = \frac{\zeta_b}{\zeta_a} \text{ on the pore surface} \tag{11}$$

$$\phi^*_1 = \frac{\zeta_b}{\zeta_a}\frac{I_0(\kappa r)}{I_0(\kappa b)} \qquad |z| \to \infty \qquad r < b \tag{12}$$

$$\mathbf{n}\cdot\nabla^*\phi^*_2 = 0 \text{ on the sphere surface} \tag{13}$$

$$\mathbf{n}\cdot\nabla^*\phi^*_2 = 0 \text{ on the pore surface} \tag{14}$$

$$\mathbf{n}\cdot\nabla^*\phi^*_2 = -E^*_z \qquad |z| \to \infty \qquad r < b \tag{15}$$

$$\mathbf{n}\cdot\nabla^* g^*_j = 0 \qquad j = 1, 2 \text{ on the sphere surface} \tag{16}$$

$$\mathbf{n}\cdot\nabla^* g^*_j = 0 \qquad j = 1, 2 \text{ on the pore surface} \tag{17}$$

$$g^*_j = -\phi^*_2 \qquad j = 1, 2 \qquad |z| \to \infty \qquad r < b \tag{18}$$

In these expressions, $E^*_z = E_z/(\zeta_a/a)$, I_0 is the zeroth-order modified Bessel function of the first kind, and ζ_b is the surface potential of the pore.

If we let p be the hydrodynamic pressure, then the flow field can be described by

$$\nabla\cdot\mathbf{v} = 0 \tag{19}$$

$$-\nabla p + \eta\nabla^2\mathbf{v} + \rho\nabla\phi = 0 \tag{20}$$

(18) O'Brien, R. W.; White, L. R. *J. Chem. Soc., Faraday Trans. 2* **1978**, *74*, 1607.

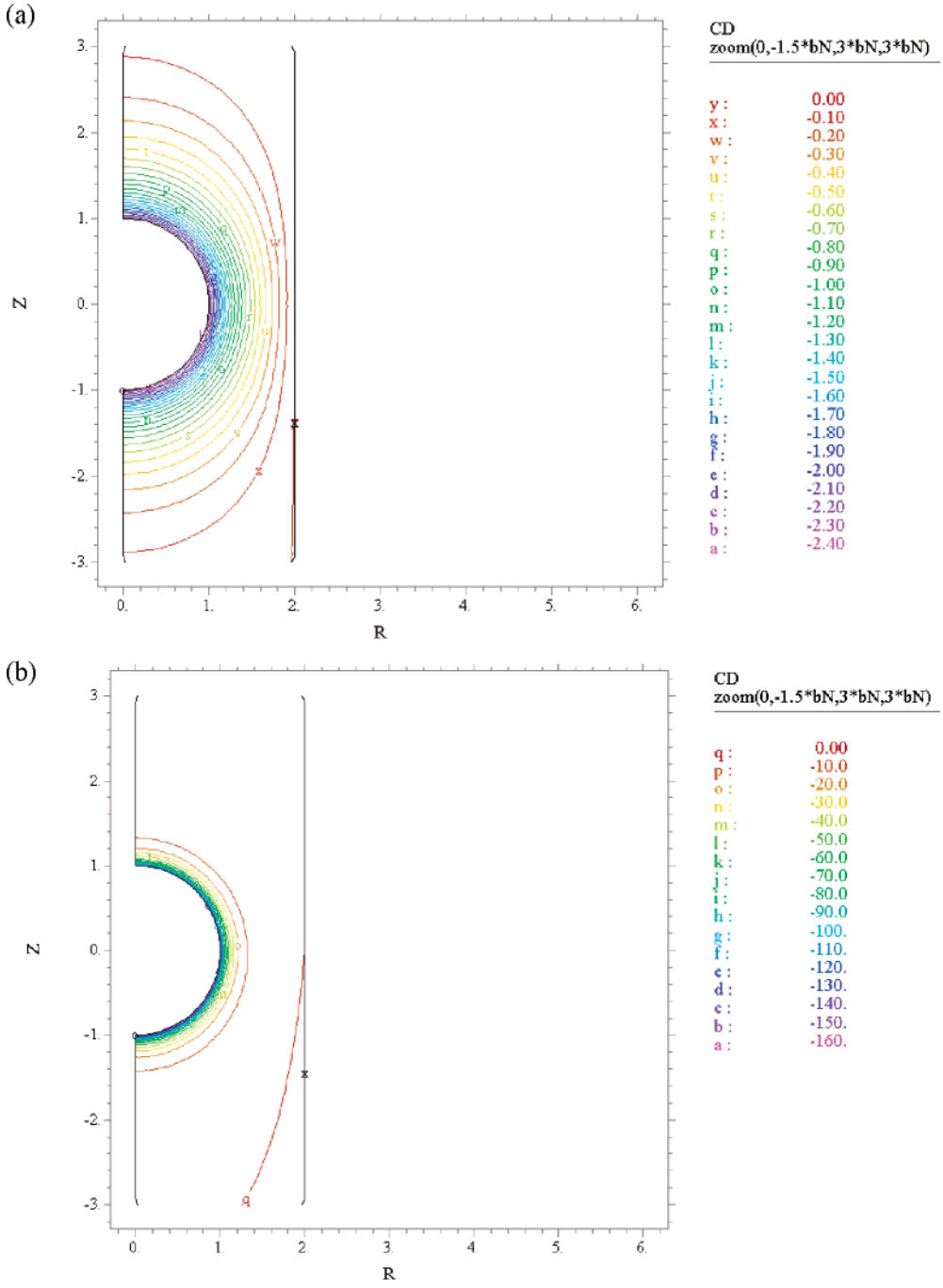

Figure 5. Contours of the net scaled ionic concentration CD ($= n^*_1 - n^*_2$) on the semiplane $\theta = \pi/2$ at two levels of ϕ_r ($= \zeta_a z_1 e/k_B T$) for the case when $\zeta_b^* = 0$, $\lambda = 0.5$, and $\kappa a = 0.8$. (a) $\phi_r = 1$ and (b) $\phi_r = 5$.

These expressions can be rewritten in scaled forms as

$$\nabla \cdot \mathbf{v}^* = 0 \tag{21}$$

$$-\nabla p^* + \nabla^2 \mathbf{v}^* + \nabla^2 \phi^* \nabla \phi^* = 0 \tag{22}$$

where $p^* = p/p_{ref}$ and $p_{ref} = \epsilon \xi_a^2/a^2$.

Assuming no-slip conditions on the surfaces of the sphere and the pore, the boundary conditions associated with eqs 21 and 22 can be expressed as

$$\mathbf{v}^* = \left(\frac{v}{U_E}\right)\mathbf{e}_z \text{ on the sphere surface} \tag{23}$$

$$\mathbf{v}^* = 0 \text{ on the pore surface} \tag{24}$$

$$\mathbf{v}^* = \left(\frac{v(r)}{U_E}\right)\mathbf{e}_z = -\left(\frac{\zeta_w}{\zeta_a}\right)\left[1 - \frac{I_0(\kappa r)}{I_0(\kappa b)}\right]\mathbf{e}_z \quad |z| \to \infty \quad r < b \tag{25}$$

Here, v is the speed of the sphere in the z direction, and $\mathbf{e}_z$ is the unit vector in the z direction. Equation 25 describes the scaled undisturbed electroosmotic velocity profile for a charged cylindrical pore in the absence of the sphere.[6]

The problem under consideration is decomposed into two subproblems.[18] In the first subproblem, a sphere moves with a constant velocity in the absence of **E**, and in the second subproblem, a sphere is fixed in space when **E** is applied. The total forces acting on a sphere in these two subproblems,

F_1 and F_2, are

$$F_1 = \chi U^* \tag{26}$$

$$F_2 = \beta E_z^* \tag{27}$$

where χ and β are constant and independent of U^* and E^*_z, respectively. Because $F_1 + F_2 = 0$ is at steady electrophoretic mobility, μ_E is given by

$$\mu_E = \frac{U^*}{E_z^*} = -\frac{\beta}{\chi} = -\frac{F_2}{F_1} \tag{28}$$

In our case, the force acting on a sphere in subproblem i, $\mathbf{F}_i$, comprises the electrical force $\mathbf{F_e}$ and the hydrodynamic force $\mathbf{F_d}$. Let F_{zi}, F_{ez}, and F_{dz} be the z components of $\mathbf{F}$, $\mathbf{F_e}$, and $\mathbf{F_d}$ in subproblem i, respectively. Then

$$F_{zi} = F_{ezi} + F_{dzi} = F_i \qquad i = 1, 2 \tag{29}$$

The axisymmetric nature of the present problem suggests that only the z components of these forces need to be considered. The electrostatic force in the z direction, F_{ez}, can be calculated by integrating the Maxwell stress tensor over the particle surface,

$$F_{ez} = \int_S (\sigma^E \cdot \mathbf{n}) \cdot \mathbf{e}_z \, dS \tag{30}$$

Here, S denotes the surface of a sphere, $\mathbf{E} = -\nabla\phi$, and $\sigma^E \equiv \epsilon(\mathbf{EE} - (1/2)\, E^2\mathbf{I})$ is the Maxwell stress tensor. It can be shown that this expression leads to[19,20]

$$F^*_{ez} = \frac{F_{ez}}{\epsilon \zeta_a^{\,2} a^2} = \int_S \frac{\partial \phi^*_1}{\partial n} \frac{\partial \phi^*_2}{\partial z} \, dS^* \tag{31}$$

where F^*_{ez} and S^* are the scaled form of F_{ez} and S, respectively (Appendix). In our case, the hydrodynamic force acting on a sphere in the z direction, F_{dz}, comprises the viscous force and the pressure and can be evaluated by[21]

$$F_{dz} = \int_S (\sigma^H \cdot \mathbf{n}) \cdot \mathbf{e}_z \, dS \tag{32}$$

where $\sigma^{\mathbf{H}} \equiv -p\mathbf{I} + \eta[\nabla\mathbf{v} + (\nabla\mathbf{v})^T]$. This expression can be rewritten in terms of scaled symbols as

$$F^*_{dz} = \frac{F_{dz}}{\epsilon \zeta_a^{\,2} a^2} = \int_S (\sigma^{*\mathbf{H}} \cdot \mathbf{n}) \cdot \mathbf{e}_z \, dS^* \tag{33}$$

where F^*_{dz} is the scaled form of F_{dz}.

The governing equations and the associated boundary conditions are solved numerically by FlexPDE,[22] a differential equation solver based on a finite element method. The applicability of this software to the resolution of the electrokinetic phenomena of the present type was justified by Hsu and Ku.[6] Double precision is used throughout the computation, and grid independence is checked to ensure that the mesh used is fine enough. In general, a convergent result can be obtained by setting the error limit of 10^{-6} for the electric field and 10^{-3} for the flow field. Two represented cases are considered in the numerical simulation, namely, a positively charged sphere is placed in an uncharged pore, and a positively charged sphere is placed in a positively charged pore.

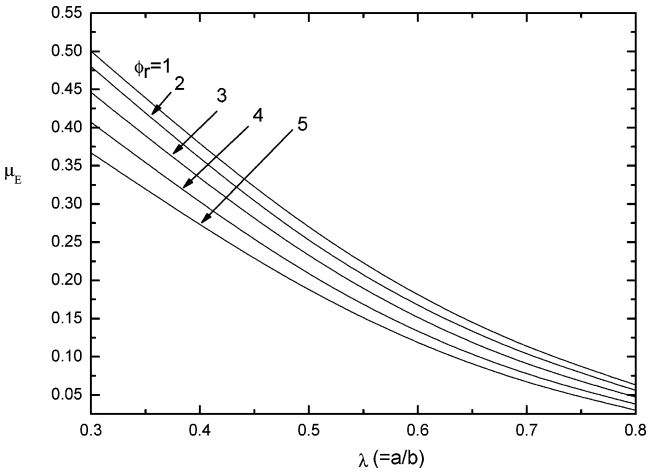

Figure 6. Variation of the scaled electrophoretic mobility μ_E (defined in eq 28) as a function of λ (= a/b) at various levels of ϕ_r (= $\zeta_a z_1 e/k_B T$) for the case when $\zeta^*_b = 0$ and $\kappa a = 1$.

3. Results and Discussion

The influences of the key parameters of the system under consideration on the electrophoretic behaviors of a sphere are examined through numerical simulation. For illustration, we assume that $a = 100$ nm and $T = 298$ K. For an aqueous solution of a common electrolyte such as KCl, we have $D_j = 2 \times 10^{-9}$ m^2/s, $\epsilon = 8.854 \times 10^{-12} \times 78.54688$ F/m, $\eta = 1$ cP, and $\alpha = 1$. These lead to $Pe_1 = Pe_2 = 0.1$. Also, we assume that a pore is sufficiently long so that the end effects of the flow field can be neglected. To make sure that this is appropriate, the transition length of a pore L_{tc}, the shortest length to achieve fully developed electroosmotic flow, is estimated under conditions of interest. The estimation of L_{tc} is based on the criteria proposed by Hsu and Kuo.[9] Figure 2a illustrates the variation of the scaled transition length of a pore (L_{tc}/a) as a function of κa for the case when both a sphere and a pore are positively charged, and that as a function of λ (= a/b) is shown in Figure 2b. According to this Figure, assuming a pore length on the order of $10a$ is sufficient to assuming a fully developed flow field.

3.1. Positively Charged Sphere in an Uncharged Pore. Let us first consider the case when a positively charged sphere is placed in an uncharged pore. The influence of the surface potential of a sphere on its mobility μ_E at various levels of double-layer thickness, measured by κa, and the boundary effect, measured by λ (= a/b), is illustrated in Figure 3. Here, the value of a is fixed, and that of κ varies, that is, we fix the radius of a sphere and let the concentration of electrolytes vary. In general, for a fixed value of κa, the higher the surface potential, the smaller the mobility; the more important the boundary effect λ, the smaller the mobility. The latter is expected because the presence of the pore wall has the effect of retarding the movement of a sphere. The former can be explained by the effect of double-layer polarization, which induces an internal electric field, the direction of which is opposite that of the applied electric field. Because the strength of the induced electric field increases with the increase in the surface potential of a sphere, μ_E decreases with the increase in the scaled surface potential of a sphere ϕ_r. Figure 3 also indicates that for a low to medium value of ϕ_r, μ_E increases with the increase in κa, and if ϕ_r is sufficiently high, then μ_E has a local minimum as κa varies. Similar phenomena were also observed by Wiersema[17] and O'Brien[18] for the electrophoresis of an isolated

(19) Hsu, J. P.; Yeh, L. H.; Ku, M. H. *J. Colloid Interface Sci.* **2007**, *305*, 324.
(20) Hsu, J. P.; Yeh, L. H. *J. Chin. Inst. Chem. Eng.* **2006**, *37*, 601.
(21) Happel, J.; Brenner, H. *Low-Reynolds Number Hydrodynamics*; Nijhoff: Boston, 1983.
(22) *FlexPDE*, version 2.22; PDE Solutions Inc.: Sunol, CA.

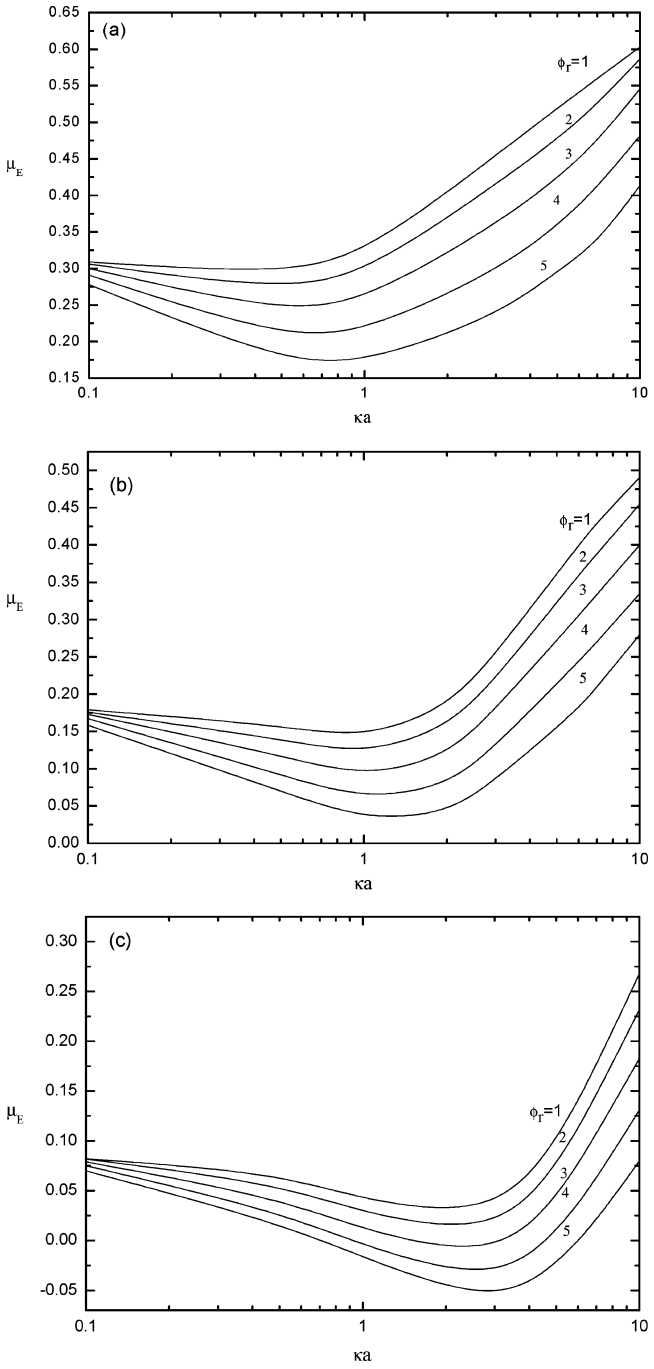

Figure 7. Variation of the scaled electrophoretic mobility μ_E (defined in eq 28) as a function of κa at various levels of ϕ_r ($= \zeta_a z_1 e/k_B T$) for the case when $\zeta^*_b = 0.2\zeta^*_a$. (a) $\lambda = 0.3$, (b) $\lambda = 0.5$, and (c) $\lambda = 0.7$.

sphere in an infinite fluid and by Lee et al.[13] for the electrophoresis of a sphere in a spherical cavity. Note that if κa is sufficiently small then μ_E becomes independent of ϕ_r.

Figure 4 shows the variations of β and F^*_{ez} as a function of the double-layer thickness measured by κa for the case presented in Figure 3 at $\lambda = 0.5$. According to the definitions, β and F^*_{ez} are measures of the net driving force and the electric force acting on a sphere in the z direction in the second subproblem, respectively. As can be seen in Figure 4, the qualitative trends in both β and F^*_{ez} are the same as that of the mobility illustrated in Figure 3.

Figure 5 illustrates the contours for the net scaled ionic concentration CD ($= n^*_1 - n^*_2$) on semiplane $\theta = \pi/2$ for two levels of the scaled surface potential of a sphere ϕ_r. This Figure

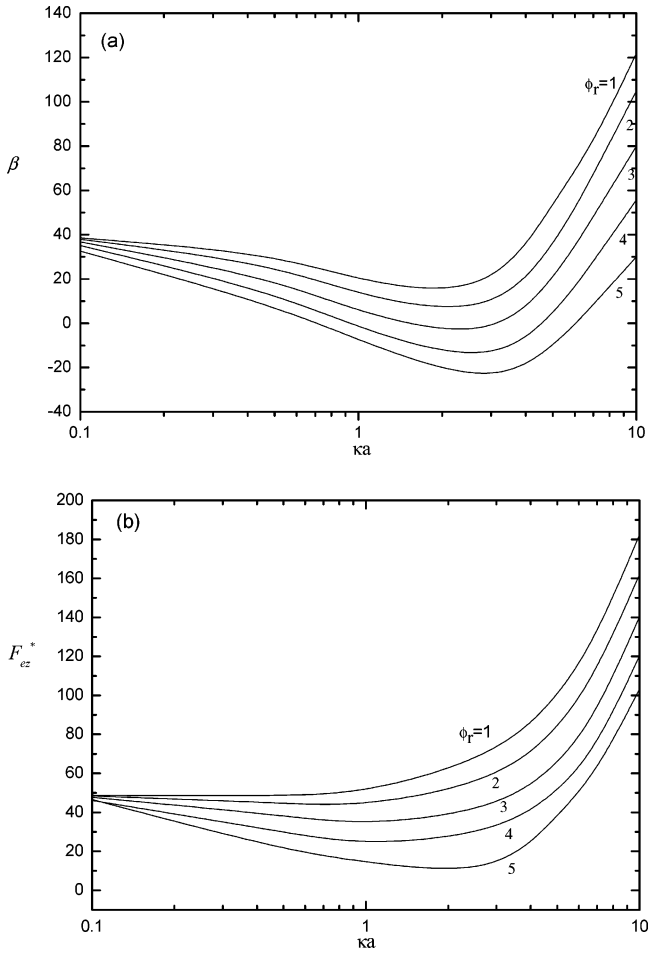

Figure 8. Variation of β (defined in eq 27) as a function of κa (a) at various levels of ϕ_r ($= \zeta_a z_1 e/k_B T$) and that of (b) F^*_{ez} (defined in eq 31) as a function of κa for the case when $\zeta^*_b = 0.2\zeta^*_a$ and $\lambda = 0.7$.

reveals that if ϕ_r is low then the contours are essentially symmetric around a sphere, implying that double-layer polarization is insignificant. On the other hand, if ϕ_r is sufficiently high, then it becomes significant. For the present case, a sphere moves upward, and the concentration of anions (counterions) near its bottom is higher than that near its top. An internal electric field is induced, the direction of which is opposite to that of the applied electric field.

The boundary effect on the mobility of a sphere for the case presented in Figure 3 at $\kappa a = 1$ is summarized in Figure 6. As mentioned previously, the more important the boundary effect, the smaller the mobility. Note that the influence of the boundary effect is threefold: the squeezing of the applied electric field between a sphere and a pore, the increase in the surface charge of a sphere due to double-layer deformation, and the increase in the viscous drag on a sphere.

3.2. Both the Sphere and Pore are Positively Charged. Consider next the case when a positively charged sphere is placed in a positively charged pore. Figure 7 shows the variation of the mobility μ_E as a function of the double-layer thickness measured by κa at various combinations of the scaled surface potential of a sphere ϕ_r and the boundary effect measured by λ ($= a/b$), and the corresponding variations of the net driving force measured by β and the scaled electric force F^*_{ez} for the case in which $\lambda = 0.7$ in the second subproblem are illustrated in Figure 8. A comparison between Figures 3 and 7 reveals that the mobility in the former is larger than that in the latter. This is because the direction of electroosmotic flow arising from the charged pore

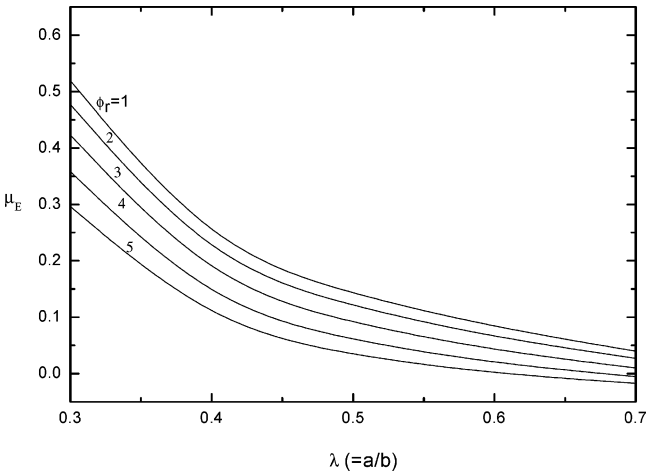

Figure 9. Variation of the scaled electrophoretic mobility μ_E (defined in eq 28) as a function of λ (= a/b) at various levels of ϕ_r (= $\zeta_a z_1 e/k_B T$) for the case when $\zeta^*_b = 0.2\zeta^*_a$ and $\kappa a = 1$.

is in the opposite direction to that of the applied electric field. The general trends in μ_E in Figure 7 are similar to that in Figure 3. However, the level of ϕ_r at which μ_E has a local minimum as κa varies in the former is lower than that in the latter. It is interesting that in Figure 7c the presence of a local minimum in μ_E may lead to two changes in sign as κa varies. The reverse direction of the electrophoresis of a sphere is interesting and can play an important role in electrophoretic measurements. The behaviors of β and F^*_{ez} shown in Figure 8 are similar to those observed in Figure 4 and can be explained by the same reasoning.

Figure 9 shows the variation in mobility μ_E as a function of the boundary effect measured by λ (= a/b) at various levels of the scaled surface potential of a sphere ϕ_r. A comparison between this Figure and Figure 6 reveals that although μ_E declines with the increase in λ in both cases as a result of the hydrodynamic retardation of the pore, μ_E is smaller in the former. This is because the movement of a sphere in the former is influenced by both the electroosmotic flow and the charge induced on its surface, and theses effects dominate its electrophoretic behavior as λ varies.

4. Conclusions

The boundary effect on electrophoresis is examined by considering the movement of a rigid sphere along the axis of a cylindrical pore at an arbitrary level of electrical potential. The effects of both double-layer polarization and electroosmotic flow arising from a charged pore are taken into account. The results of numerical simulation can be summarized as follows. For a positively charged sphere in an uncharged pore, if the surface potential of the sphere is high, then its mobility has a local minimum as the thickness of its double layer varies, which is of practical significance, For example, if capillary electrophoresis is used as a separation tool, then the bulk electrolyte concentration needs to be selected carefully to prevent minimum efficiency. For a fixed double-layer thickness, the mobility decreases with the increases in the surface potential. In general, the presence of the pore wall has the effect of reducing the mobility of a sphere. For the case when both a sphere and a pore are positively charged, the mobility of the sphere may also have a local minimum as the thickness of its double layer varies even if its surface potential is low. Depending upon the level of the surface potential of a sphere, the direction of its movement may change twice as the thickness of its double layer varies, which is a result of practical significance, for example, when capillary electrophoresis is chosen as a separation tool. In this case, the separation efficiency depends largely upon the bulk concentration of electrolytes.

Appendix: Derivation of Equation 31[19,20]

For convenience, eq 30 is written as

$$F_{ez} = \int\int_S (\sigma^E \cdot \mathbf{n}) \cdot \mathbf{e}_z \, dS \tag{A1}$$

where $\sigma^E \equiv \epsilon(\mathbf{EE} - (1/2)\, E^2\mathbf{I})$ and $\mathbf{E} = -\nabla\phi = \mathbf{n}(\partial\phi/\partial n) + \mathbf{t}(\partial\phi/\partial t)$. Here, $\mathbf{I}$ is the unit tensor, $\mathbf{t}$ is the unit tangential vector on the particle surface, n and t are the magnitudes of $\mathbf{n}$ and $\mathbf{t}$, respectively, and $E^2 = \mathbf{E}\cdot\mathbf{E}$. Substituting σ^E into eq A1 yields

$$F_{ez} = \int\int_S \left(\epsilon \frac{\partial\phi}{\partial n}\frac{\partial\phi}{\partial z} - \frac{1}{2}\epsilon\left[\left(\frac{\partial\phi}{\partial n}\right)^2 + \left(\frac{\partial\phi}{\partial t}\right)^2\right] n_z\right) dS \tag{A2}$$

where n_z is the z component of $\mathbf{n}$. Because $\phi = \phi_1 + \phi_2$, eq A2 becomes, after eliminating some minor terms,

$$F_{ez} = \int\int_S \left(\epsilon \frac{\partial\phi_1}{\partial n}\frac{\partial\phi_2}{\partial z} + \frac{\partial\phi_2}{\partial n}\frac{\partial\phi_1}{\partial z} - \epsilon\left[\frac{\partial\phi_1}{\partial n}\frac{\partial\phi_2}{\partial n} + \frac{\partial\phi_1}{\partial t}\frac{\partial\phi_2}{\partial t}\right] n_z\right) dS \tag{A3}$$

For the present case, because the sphere is nonconducting,

$$\int\int_S \epsilon\left[\left(\frac{\partial\phi_2}{\partial n}\frac{\partial\phi_1}{\partial z}\right) - \left(\frac{\partial\phi_1}{\partial n}\frac{\partial\phi_2}{\partial n}\right) n_z\right] dS$$

vanishes, and eq A3 reduces to

$$F_{ez} = \int\int_S \left(\epsilon\left[\frac{\partial\phi_1}{\partial n}\frac{\partial\phi_2}{\partial z}\right] - \epsilon\left[\frac{\partial\phi_1}{\partial t}\frac{\partial\phi_2}{\partial t}\right] n_z\right) dS \tag{A4}$$

If the surface of a particle is maintained at a constant potential, then $\partial\phi_1/\partial t = 0$, and this expression can be further simplified to

$$F_{ez} = \int\int_S \epsilon\frac{\partial\phi_1}{\partial n}\frac{\partial\phi_2}{\partial z}\, dS \tag{A5}$$

Rewriting this equation with scaled symbols leads to eq 31 in the text.

Acknowledgment. This work is supported by the National Science Council of the Republic of China.

LA070079M